



Minerva Access is the Institutional Repository of The University of Melbourne

Author/s:

Lu, C;Zanker, D;Lock, P;Jiang, X;Deng, J;Duan, M;Liu, C;Faou, P;Hickey, MJ;Chen, W

Title:

Memory regulatory T cells home to the lung and control influenza A virus infection

Date:

2019-10-01

Citation:

Lu, C., Zanker, D., Lock, P., Jiang, X., Deng, J., Duan, M., Liu, C., Faou, P., Hickey, M. J. & Chen, W. (2019). Memory regulatory T cells home to the lung and control influenza A virus infection. *Immunology and Cell Biology*, 97 (9), pp.774-786. <https://doi.org/10.1111/imcb.12271>.

Persistent Link:

<https://hdl.handle.net/11343/285959>

1  
2  
3  
4  
5  
6  
7  
8  
9  
10  
11  
12  
13  
14  
15  
16  
17  
18  
19  
20  
21  
22

PROFESSOR MICHAEL HICKEY (Orcid ID : 0000-0003-2354-357X)

PROFESSOR WEISAN CHEN (Orcid ID : 0000-0002-5221-9771)

Article type : Original Article

### **Memory regulatory T cells home to the lung and control influenza A virus infection**

Chunni Lu<sup>1</sup>, Damien Zanker<sup>1</sup>, Peter Lock<sup>1</sup>, Xiangrui Jiang<sup>1</sup>, Jieru Deng<sup>1</sup>, Mubing Duan<sup>1</sup>,  
Chuanxin Liu<sup>1</sup>, Pierre Faou<sup>1</sup>, Michael J Hickey<sup>2</sup> and Weisan Chen<sup>1,3</sup>

<sup>1</sup>La Trobe Institute for Molecular Science, School of Molecular Science, La Trobe University,  
Bundoora, VIC, Australia.

<sup>2</sup>Centre for Inflammatory Diseases, Monash University Department of Medicine, Monash  
Medical Centre, Clayton, VIC, Australia.

**Running title: Memory Tregs control influenza A virus infection in the lung**

**Keywords:** Influenza A virus, infection-experienced, memory regulatory T cells, C57BL/6

This is the author manuscript accepted for publication and has undergone full peer review but has not been through the copyediting, typesetting, pagination and proofreading process, which may lead to differences between this version and the [Version of Record](#). Please cite this article as [doi: 10.1111/IMCB.12271](https://doi.org/10.1111/IMCB.12271)

This article is protected by copyright. All rights reserved

23 <sup>3</sup>To whom correspondence should be addressed: [weisan.chen@latrobe.edu.au](mailto:weisan.chen@latrobe.edu.au)

24

## 25 **ABSTRACT**

26 Memory regulatory T cells (mTregs) have been demonstrated to persist long-term in hosts after  
27 the resolution of primary influenza A virus (IAV) infection. However, whether such IAV  
28 infection-experienced (IAV-experienced) mTregs differentiate into a phenotypically and  
29 functionally distinct Treg subset and what function they play at the infection site remain poorly  
30 defined. In this study, we characterized the phenotype, examined the responsiveness and  
31 assessed the suppressive function of IAV-experienced mTregs. In comparison with  
32 inexperienced naïve Tregs (nTregs), mTregs exhibited elevated expression of CD39, CD69,  
33 CD103, CTLA-4, LFA-1 and PD-1 and could be activated in an antigen-specific manner *in vitro*  
34 and *in vivo*. When mTregs and nTregs were adoptively co-transferred into recipient mice,  
35 mTregs had a competitive advantage in migrating to the IAV infected lungs. mTregs were more  
36 capable of controlling *in vitro* proliferation of CD4<sup>+</sup> and CD8<sup>+</sup> T cells and suppressed CD40 and  
37 CD86 upregulation on bone marrow-derived dendritic cells (BMDCs). Adoptively transferred  
38 mTregs, but not nTregs, significantly attenuated body weight loss, lung pathology and immune  
39 cell infiltration into the infected lungs. These results suggest that mTregs generated after IAV  
40 infection differentiate into a phenotypically distinct and functionally enhanced Treg subset that  
41 can be activated in an antigen-specific manner to exert immunosuppression. We propose  
42 vaccination to induce such mTregs as a potential novel strategy to protect against severe IAV  
43 infection.

44

45

## 46 **INTRODUCTION**

47 Regulatory T cells (Tregs) expressing the X-chromosome-encoded transcription factor Foxp3  
48 represent a specialized lineage of T lymphocytes with prominent immunosuppressive function.<sup>1,2</sup>  
49 Tregs were initially discovered as a key immunoregulator of autoimmunity, maintaining self-  
50 tolerance via suppressing autoreactive T cells that have escaped negative selection in thymus.<sup>3,4</sup>

51 Imbalance between Tregs and autoreactive T cells, impaired Treg proliferation capacity or  
52 defects in Treg suppressive function may therefore lead to the development of a variety of  
53 autoimmune diseases.<sup>5-8</sup> In addition to the maintenance of immune tolerance to self-antigens,  
54 Tregs are involved in modulating immune responses to acute microbial pathogens. For example,  
55 during acute infection by respiratory syncytial virus (RSV) and herpes simplex virus (HSV),  
56 Tregs are critical in limiting the infection-induced innate and adaptive immune responses and the  
57 corresponding tissue inflammation at the infection sites.<sup>9-12</sup>

58 Tregs have been investigated in acute influenza A virus (IAV) infection in recent years. It has  
59 become clear that, following primary IAV infection, Tregs can be activated by IAV-derived  
60 peptides and the activated Tregs are widely disseminated in the lung and lung-draining  
61 mediastinal lymph node (mLN) and, to a lesser extent, in the spleen and peripheral non-draining  
62 lymph node (pLN).<sup>13, 14</sup> Importantly, after the resolution of primary IAV infection, Tregs could  
63 maintain within the host to become long-lived memory Tregs (mTregs).<sup>15</sup> However, whether  
64 such IAV-infection experienced (IAV-experienced) mTregs represent a distinct Treg subset that  
65 differs from the inexperienced naïve Tregs (nTregs) in their phenotypes and their roles during  
66 subsequent IAV infection are largely unclear. The persistence of IAV-experienced mTregs in the  
67 host may point to a potential vaccination strategy, inducing a pool of IAV-experienced mTregs  
68 to target a wide range of IAV infection-induced detrimental cellular immune responses. However,  
69 the therapeutic efficacy of such IAV-experienced mTreg remains to be determined.

70 In this study, we sought to address these questions by deciphering the phenotype and examining  
71 the responsiveness and suppressive capacity of IAV-experienced mTregs. Considering that the  
72 appropriate localization of Tregs at the infection site is essential for them to interact with and  
73 modulate their cellular targets,<sup>16</sup> we also evaluated the ability of IAV-experienced mTregs to  
74 migrate into the infected lungs and their effects on IAV infection-induced pulmonary cellular  
75 immune responses. We found that mTregs exhibited elevated expression of cell migration- and  
76 function-associated molecules relative to nTregs. Upon activation *in vitro*, mTregs displayed  
77 enhanced proliferation and cytokine production capacity compared to nTregs. In response to IAV  
78 infection *in vivo*, mTregs were highly activated, proliferative and showed competitive advantage  
79 in migrating to the infection site in comparison with nTregs. Importantly, mTregs could  
80 effectively attenuate lung pathology, limit pulmonary immune cell infiltration and control

81 ongoing antigen-specific T cell responses in the lungs. These data suggest that mTregs generated  
82 in the setting of IAV infection have differentiated into a population with distinct phenotype,  
83 enhanced responsiveness and peripheral infection-site migratory capacity which give rise to their  
84 control of IAV infection.

85

## 86 **RESULTS**

### 87 *mTregs display distinct phenotype and are more responsive to IAV than nTregs in vitro*

88 Knowing that a pool of mTregs can be differentiated and maintained in the host after the  
89 resolution of primary IAV infection,<sup>15</sup> we questioned whether mTregs are phenotypically  
90 different from their naïve counterparts. To address this question, we analyzed the phenotype of  
91 nTregs and mTregs from various tissues including spleen, peripheral non-draining inguinal  
92 lymph node (pLN), lung-draining mediastinal lymph node (mLN) and lung of IAV-infected mice.  
93 Considering that the bulk of mTregs may contain a small fraction of Tregs with CD44<sup>+</sup>CD62L<sup>-</sup>  
94 <sup>/low</sup> phenotype that was also found in naïve mice,<sup>17</sup> we therefore included Tregs with  
95 CD44<sup>+</sup>CD62L<sup>-/low</sup> expression from age/sex matched naïve mice, termed them as “nmTregs”, as  
96 control. We assessed the expression of surface molecules associated with cell activation,  
97 proliferation and migration, including CD25, CD39, CD69, CD103, cytotoxic T lymphocyte-  
98 associated antigen-4 (CTLA-4), leukocyte function-associated antigen-1 (LFA-1), programmed  
99 cell death-1 (PD-1) and Foxp3. Our results showed that the expression levels of Foxp3 on nTregs  
100 and mTregs were similar, whereas the CD25 expression on mTregs was slightly lower (Figure 1).  
101 Noteworthy, mTregs exhibited elevated expression of an array of cell migration- and  
102 suppressive function-associated molecules, including CD39, CD69, CD103, CTLA-4, LFA-1  
103 and PD-1 (Figure 1). Thus, mTregs represent a distinct Treg population.

104 We further determined whether mTregs could actively respond to IAV *in vitro* by investigating  
105 cell activation and proliferation marked by Ki67 expression. Nearly 38% mTregs stimulated with  
106 IAV-infected BMDCs expressed Ki67, but only 10% of nTregs expressed Ki67 (Figure 2a).  
107 Moreover, tracking nTregs and mTregs via time-lapse live cell imaging revealed that, after being  
108 co-cultured with IAV-infected BMDCs, mTregs but not nTregs displayed frequent change in cell  
109 morphology and made more contact with IAV-infected BMDCs (Figure 2b and Supplementary

110 figure 1a and b), which suggests that mTregs were more activated and more mobile than nTregs.  
111 To show the lack of nTreg response was not an intrinsic defect in these cells, we stimulated both  
112 mTregs and nTregs using anti-CD3/CD28 mAbs and more than 90% mTregs and nTregs  
113 expressed the proliferation marker Ki67 (Supplementary figure 2), indicating these Tregs are  
114 equally capable of responding to TCR stimulation.

115

116 *mTregs are highly activated and proliferative upon IAV infection with an enhanced infection*  
117 *site-migration capacity*

118 We next sought to understand the extent to which mTregs differ from their naïve counterparts in  
119 responding to IAV *in vivo*. We co-transferred mTregs isolated from IAV-immunized C57BL/6  
120 Foxp3<sup>eGFP</sup> mice and nTregs isolated from uninfected C57BL/6 mice into congenic Ly5.1  
121 recipients (Figure 3a), so that the responsiveness of mTregs and nTregs to IAV could be directly  
122 compared in the same environment. The recipients were intranasally infected with IAV 12 h after  
123 co-transfer. The distribution, activation and proliferation of the adoptively co-transferred mTregs  
124 (eGFP<sup>+</sup> and CD45.2<sup>+</sup>) and nTregs (eGFP<sup>-</sup> and CD45.2<sup>+</sup>) were investigated 10 days post infection  
125 (dpi) (Figure 3b). At 10 dpi, both the co-transferred mTregs and nTregs were detected in the  
126 spleens, pLNs, mLNs, BALs and lungs of the recipients. However, mTregs were highly activated  
127 and more proliferative than nTregs in all of the analyzed tissues based on Ki67<sup>+</sup> cell proportion  
128 (Figure 3c). Moreover, the proportions of mTregs were higher than that of nTregs in the spleens  
129 and much more so in the BALs (93% vs 7%) and lungs (86% vs 14%) (Figure 3d). These  
130 observations were consistent with their numbers in all analyzed tissues, with higher number of  
131 mTregs than nTregs in the spleens, BALs and lungs and comparable numbers of both  
132 populations in the pLNs and mLNs (Figure 3e). Thus, mTregs are specifically activated *in vivo*  
133 upon exposure to IAV and have a competitive advantage in migrating to and proliferating at the  
134 infection site during IAV infection, which was further supported by the lack of proliferation and  
135 much lower migration number in the above-mentioned sites when transferred mTregs were  
136 tracked in mice treated with PBS (Supplementary figure 3).

137

138 *mTregs are more capable of inhibiting T cell proliferation and modulating BMDC costimulatory*  
139 *function in vitro than nTregs*

140 We next assessed the suppressive capacity of these various Treg subsets *in vitro* in a CD4<sup>+</sup> or  
141 CD8<sup>+</sup> T cell proliferation assay. Infected antigen presenting cells are considered as a more  
142 physiological APC to evaluate Treg suppression<sup>15</sup>. Thus, mTregs or nTregs were cocultured  
143 with IAV-specific CD4<sup>+</sup> and CD8<sup>+</sup> T cells stimulated by IAV-infected BMDCs. Our results  
144 showed that both IAV-specific CD4<sup>+</sup> and CD8<sup>+</sup> T cells were highly proliferative when they were  
145 stimulated with IAV-infected BMDCs in the absence of mTregs or nTregs (Figure 4a and b).  
146 When mTregs or nTregs were added into the co-cultures, the proliferation of IAV-specific CD4<sup>+</sup>  
147 and CD8<sup>+</sup> T cells were significantly inhibited (Figure 4c). Suppressive effects of nTregs and  
148 mTregs closely correlated with Treg/responder T cell ratio, with increased suppression on IAV-  
149 specific CD4<sup>+</sup> and CD8<sup>+</sup> T cell proliferation at higher Treg/responder T cell ratios. In comparison  
150 to nTregs, mTregs displayed 2~4 fold enhanced suppression on IAV-specific CD4<sup>+</sup> and CD8<sup>+</sup> T  
151 cell proliferation on a per cell basis (Figure 4c). Thus, mTregs are more capable of suppressing  
152 IAV-specific CD4<sup>+</sup> and CD8<sup>+</sup> T cells proliferation.

153 We also examined whether mTregs could regulate the T cell stimulatory function of BMDCs by  
154 analyzing their expression of core functional molecules, CD40, CD86 and MHC-II. BMDCs co-  
155 cultured with IAV-specific CD4<sup>+</sup> T cells in the presence of IAV showed dramatic upregulation in  
156 their co-stimulatory molecule CD40 and CD86 expression compared with control BMDCs  
157 cultured in medium alone (Figure 5a and b). However, such co-stimulatory molecule  
158 upregulation was dramatically reduced when mTregs were added into the co-cultures (Figure 5a  
159 and b), nTregs showed significantly less suppression on CD40 and CD86 expression compared  
160 to mTregs (Figure 5a and b). Notably, the evident up- or down-regulation of CD40 and CD86 on  
161 BMDCs were observed only when BMDCs were co-cultured with CD4<sup>+</sup> T cells or CD4<sup>+</sup> T cells  
162 plus Tregs, respectively, in the presence of IAV, as there was no significant increase in CD40 or  
163 CD86 expression on BMDCs cultured in the presence of IAV compared to BMDCs cultured in  
164 medium alone (Supplementary figure 4a and b). MHC-II expression on BMDCs was not altered  
165 either co-cultured with or without T cells, plus or minus nTregs or mTregs (data not shown).  
166 Collectively, these data suggest that mTregs actively control T cell costimulation function of

167 BMDCs through suppressing their CD40 and CD86 up-regulation, and such control by mTregs is  
168 more potent than that by nTregs.

169

170 *mTregs effectively attenuate IAV infection-induced body weight loss and lung pathology*

171 We next sought to define a role for mTregs *in vivo* during IAV infection. Intranasal infection  
172 with a sublethal dose of IAV generally result in body weight loss and lung tissue damage in mice.  
173 In our study, mice that were intranasally infected by a sublethal dose of PR8 displayed a  
174 progressive reduction in body weight between 3-9 days post infection (Figure 6a, “Infected”).  
175 Moreover, histopathological analysis and histology scoring of the infected lungs at 10 dpi  
176 revealed extensive cell infiltration in the lung parenchyma and a markedly increased severity of  
177 overall lung pathology compared to the uninfected lungs (Figure 6a and c, “Infected only”).  
178 Interestingly, however, the adoptively transferred mTregs actively attenuated infection-induced  
179 body weight loss, coupled with an earlier recovery of body weight from day 8 post infection  
180 (Figure 6a, blue line). The presence of adoptively transferred mTregs also significantly  
181 attenuated the prominent lung immune cell infiltration and pathology (Figure 6b and c, “Infected  
182 + mTregs”). To account for a potential contribution of nTregs, we also infected recipient mice  
183 received adoptively transferred nTregs. Nevertheless, under the same conditions, nTregs failed to  
184 ameliorate such infection-induced body weight loss (Figure 6a, “Infected + nTregs”) and lung  
185 pathology (Figure 6b and c, “Infected + nTregs”). Thus, these data together demonstrate a key  
186 role for mTregs in controlling IAV infection-induced body weight loss and mediating tissue  
187 protection during IAV infection.

188

189 *mTregs selectively limit the infiltration of monocytes and neutrophils into the infected lungs*

190 To understand how mTregs contribute to the control of IAV infection-induced lung pathology,  
191 we analyzed the infiltrating cells in the lungs of mice that had or had not received mTregs.  
192 During IAV infection, while innate and adaptive immune cells rapidly orchestrate antiviral  
193 immune responses to control the infection, they may also act deleteriously to initiate or  
194 exacerbate the production of pro-inflammatory cytokines and chemokines, reactive oxygen  
195 species and nitric oxide that may lead to lung tissue injury.<sup>18, 19</sup> Therefore, we analyzed the lung-

196 infiltrating monocytes, interstitial macrophages, neutrophils, IFN- $\gamma$ -secreting CD4<sup>+</sup> and CD8<sup>+</sup> T  
197 cells at 10 dpi. Our results showed that IAV infection led to a dramatic increase of the infiltration  
198 of these cell types into the lungs (Supplementary figure 5, “Infected only”). However, in mice  
199 that received mTreg transfer, IFN- $\gamma$ -secreting CD4<sup>+</sup> and CD8<sup>+</sup> T cell infiltration was markedly  
200 reduced, and monocyte and neutrophil infiltration was significantly reduced (Supplementary  
201 figure 5, “Infected + mTregs”). In mice that received nTregs, such infiltration was largely  
202 unaffected (Supplementary figure 5, “Infected + nTregs”). Collectively, these data suggest that  
203 mTregs mediate lung tissue protection most likely by limiting immune cell infiltration, especially  
204 monocytes and neutrophils, into the lung.

205

## 206 **DISCUSSION**

207 We showed in this study that IAV-experienced mTregs belong to a distinct Treg subset. In fact,  
208 our study provides the first comprehensive phenotyping of IAV-experienced mTregs. We further  
209 demonstrated that IAV-experienced mTregs, but not nTregs, are more responsive *in vitro* to  
210 IAV-infected APCs and able to suppress the upregulation of BMDC costimulation molecules;  
211 and that *in vivo* they are more capable of migrating into IAV infection site, proliferating  
212 vigorously, suppressing innate and adaptive immune cell infiltrating into the infected lungs, and  
213 most importantly attenuating lung pathology caused by IAV infection reflected by both much  
214 milder histological changes and significantly decreased body weight loss.

215

216 A previous study investigating Treg regulation of memory CD8<sup>+</sup> T cell response to secondary  
217 IAV infection revealed the long-term existence of mTregs in the host.<sup>15</sup> However, the  
218 phenotypical difference between IAV-experienced mTregs and their naïve counterparts is not  
219 well established. We have shown in this study that the expression of CD39, CD69, CD103,  
220 CTLA-4, LFA-1 and PD-1 is upregulated in mTregs as opposed to nTregs, providing further  
221 evidence for the previously identified mTregs in the setting of IAV infection that IAV-  
222 experienced mTregs have differentiated into a phenotypically distinct subset of Tregs.

223 Tregs become activated in response to IAV infection and were shown to play an important role  
224 in modulating immune responses to primary IAV infection,<sup>14, 20, 21</sup> and mTregs were shown to be

225 more capable of suppressing pulmonary CD8<sup>+</sup> T cell response during secondary IAV infection  
226 than nTregs.<sup>15</sup> Interestingly, the factors that contribute to such enhanced immunosuppression of  
227 mTregs during IAV infection remain poorly understood as both nTregs and mTregs should have  
228 similar suppression capacity on a per cell basis.<sup>22</sup> However, since Tregs must be activated to  
229 exert their suppressive function,<sup>23</sup> one possible mechanism is that mTregs are able to recognize  
230 previously encountered antigens. This may confer an enhanced ability of mTregs to search and  
231 interact with APCs bearing previously encountered IAV antigens for activation and proliferation,  
232 especially at the infection site. In support for this, we compared the responsiveness of mTregs  
233 and nTregs *in vitro* and *in vivo* and found that mTregs, but not nTregs, were highly activated *in*  
234 *vitro* after stimulation with IAV-infected BMDCs. Time-lapse live cell imaging also showed that  
235 mTregs were more capable of interacting with IAV-infected BMDCs. Moreover, in IAV-infected  
236 recipient mice, significantly more transferred mTregs were activated than nTregs in all analyzed  
237 tissues, including spleens, pLNs, mLNs, BALs and, especially in the lungs. Such activation was  
238 largely antigen-specific as only a small fraction of the transferred mTregs were activated in the  
239 uninfected recipients. Another possible mechanism could be the mTregs' enhanced infection  
240 site-migration capacity. There is increasing evidence indicating that appropriate Treg migration  
241 is essential for them to interact with and modulate their cellular targets. For example, CD62L  
242 expressing Tregs were especially potent at entering lymph nodes to suppress proliferation of self-  
243 antigen- and alloantigen-specific T cells, thereby suppressing autoimmunity and graft rejection,  
244 respectively.<sup>24, 25</sup> In contrast, CD103 expressing Tregs displayed poor capacity in migrating to  
245 lymph nodes but were exclusively recruited to skin to control *Leishmania* major infection and  
246 antigen-induced arthritis.<sup>26, 27</sup> The elevated expression of CD103 on mTregs, relative to that on  
247 nTregs, therefore indicate an enhanced infection site-migration capacity of mTregs. Consistent  
248 with this possibility, after adoptive co-transfer, we found significantly more mTregs than nTregs  
249 in the BALs and lungs of infected recipients at 10 dpi.

250 Two mechanisms may be involved in mTregs-mediated attenuation of lung pathology and body  
251 weight loss. Firstly, this could be the outcome of decreased pulmonary immune cell infiltration  
252 as in mice that had received mTregs the infiltrating monocytes, neutrophils and IFN- $\gamma$ -producing  
253 CD4<sup>+</sup> and CD8<sup>+</sup> T cells were significantly reduced. These cells secreted proinflammatory  
254 cytokines such as TNF- $\alpha$ , IL-1 $\beta$  and IL-6 following IAV infection,<sup>19</sup> and they were reported to  
255 contribute to "cytokine storm".<sup>28-30</sup> Since monocytes are the major source of chemoattractant

256 MIP-1 $\alpha$ , MCP-1 and IP-10<sup>31</sup>, the suppression of pulmonary infiltration of monocytes by mTregs  
257 may prevent recruitment of additional immune cells to the infected lungs, thereby the  
258 exacerbation of lung pathology. Secondly, the higher expression of CD39 by mTregs may  
259 contribute to tissue protection. In support of this conclusion, CD39 expressed by Tregs was  
260 shown to induce the production of immunosuppressive adenosine through hydrolyzing  
261 proinflammatory ATP, thereby controlling IL-17 mediated autoimmune inflammation and the  
262 secretion of proinflammatory cytokine IL-1 $\beta$ .<sup>32, 33</sup>

263 We observed that there were significant reductions in the numbers of IFN- $\gamma$ -producing CD4<sup>+</sup> and  
264 CD8<sup>+</sup> T cells in the infected lungs of mice that had adoptively transferred mTregs. Such  
265 suppression of IFN- $\gamma$ -producing CD4<sup>+</sup> and CD8<sup>+</sup> T cell responses in the lungs by mTregs may be  
266 mediated by modifying the antigen-presentation capacity of local APCs. It has been reported that  
267 additional antigen presentation by pulmonary APCs, including plasmacytoid DCs, CD8 $\alpha$ <sup>+</sup> DCs  
268 and interstitial DCs, sustains antigen-specific T cell responses in the infected lungs.<sup>34</sup> However,  
269 CTLA-4 expressed by Tregs was demonstrated to limit T cell priming and proliferation via  
270 suppressing co-stimulation function of DCs.<sup>35, 36</sup> In addition, aggregation of Tregs on DCs in an  
271 LFA-1 dependent-manner also led to a lethargic state of DCs, thereby a reduced T cell priming.<sup>37</sup>  
272 We also observed that mTregs had markedly elevated expression of CTLA-4 and LFA-1  
273 compared to nTregs. More importantly, mTregs could actively down-regulate CD40 and CD86  
274 expression on BMDCs. Therefore, mTregs may actively act on pulmonary APCs leading to the  
275 inhibition of excessive antigen-specific CD4<sup>+</sup> and CD8<sup>+</sup> T cell responses.

276 Taken together, using an adoptive Treg transfer approach, rather than CD25<sup>+</sup> Treg depletion, we  
277 demonstrate an IAV-experienced mTreg population, likely containing polyclonal IAV-specific  
278 mTregs, was able to reduce IAV-infection associated lung pathology and body weight loss. Our  
279 study model resembles a preventative vaccination scenario in which an antigen-specific mTreg  
280 pool was established before the host was IAV infected. IAV-specific mTregs can be induced  
281 after vaccination with UV-inactivated IAV or vaccines containing specific IAV peptides,  
282 although such Tregs may dampen the effector T cell response a little.<sup>38, 39</sup> It is possible and likely  
283 helpful that for future IAV vaccines to incorporate specific strategies to stimulate some IAV-  
284 specific mTregs. It would be more appealing if such vaccine is given via the intranasal route and  
285 induces lung-resident mTregs as intranasal administration but not injection of influenza vaccines

286 are more expected to improve the efficacy of influenza vaccines and generating lung-resident  
287 memory T cells.<sup>40, 41</sup> Such IAV-specific mTregs or lung-resident mTregs might provide more  
288 timely immune regulation at the infection sites to minimize IAV infection-caused  
289 immunopathology without significantly affecting immune protection provided by both innate and  
290 adaptive immune cells.

291

## 292 **METHODS**

### 293 *Mice*

294 Female C57BL/6 and Ly5.1 mice were purchased from the Walter Eliza Hall Institute of Medical  
295 Research (Melbourne, Australia). B6-Foxp3<sup>eGFP</sup> mice, on a C57BL/6 background,<sup>42</sup> were kindly  
296 provided by Dr. Alexander Y. Rudensky (Memorial Sloan Kettering Cancer Center, New York,  
297 NY) and bred in house. Mice were housed under specific pathogen free (SPF) conditions in the  
298 animal facility at La Trobe University. All animal experiments were approved by the La Trobe  
299 University Animal Ethics Committee and performed in accordance with the National Health and  
300 Medical Research Council guidelines.

301

### 302 *Influenza A viruses and infections*

303 Influenza A virus PR8 (A/Puerto Rico/8/34, H1N1) was obtained from Lorena Brown  
304 (University of Melbourne, Australia) and X-31 (A/X-31, H3N2) from Jonathan Yewdell (NIH,  
305 USA). New viral stocks of PR8 and X-31 were propagated in 10-day-old embryonated chicken  
306 eggs, titered and stored as previously described.<sup>43</sup> For *in vivo* primary infection, 9~10-week-old  
307 mice were anesthetized with methoxyflurane and intranasally infected with 70 pfu of PR8 (in 30  
308  $\mu$ l PBS). For *in vivo* secondary infection, mice were firstly infected by 70 pfu of PR8 and  
309 challenged 35 days later with 10<sup>4</sup> pfu of X-31 (in 30  $\mu$ l PBS). For *in vitro* infection, 1~3 x 10<sup>6</sup>  
310 cells were co-incubated with a 10 multiplicity of infection (MOI) dose of PR8 for 1 h in 200  $\mu$ l  
311 AIM medium (RPMI-1640 medium supplemented with HCl to pH 6.0), followed by 12 h in 2  
312 mL complete medium, RPMI-1640 medium supplemented with 10% fetal calf serum (FCS), at  
313 37°C, 5% CO<sub>2</sub>.

314

315 *Tissue harvest and cell isolation*

316 Mice were sacrificed at indicated time points and cells were isolated from the spleens, lymph  
317 nodes, lung airways and lung parenchyma. Spleens were mechanically disrupted in incomplete  
318 medium (RPMI-1640 medium supplemented with 2% FCS). Lymph nodes were mechanically  
319 disrupted in incomplete medium containing 5mM EDTA. Bronchoalveolar lavage (BAL) cells  
320 were collected by four instillations of BAL with 0.5 mL incomplete medium. Cells from the lung  
321 parenchyma were isolated by digestion with collagenase A and DNase I (1 mg mL<sup>-1</sup> and 0.2mg  
322 mL<sup>-1</sup>, respectively, Roche, Switzerland) at room temperature (RT) for 25 min prior to being  
323 passed through a nylon mesh. After red blood cell (RBC) lysis, cells were resuspended in  
324 complete medium before use.

325

326 *Peptide stimulation*

327 For *ex vivo* analysis of IFN- $\gamma$  production by CD4<sup>+</sup> and CD8<sup>+</sup> T cells in the lungs, the cells  
328 isolated from the lungs were stimulated with peptides (HA<sub>211-225</sub>, NP<sub>311-325</sub>, PB2<sub>106-120</sub>, and PA<sub>465-</sub>  
329 <sub>470</sub>, 10<sup>-5</sup> M, for CD4<sup>+</sup> T cell stimulation; NP<sub>366-374</sub>, PA<sub>224-233</sub>, PB1<sub>703-711</sub> and PB2<sub>196-206</sub>, 10<sup>-8</sup> M, for  
330 CD8<sup>+</sup> T cell stimulation) for 5 h in the presence of BFA at 37°C, 5% CO<sub>2</sub>.

331

332 *Cell staining and Flow cytometry*

333 For cell surface marker staining, cells were incubated with Fc block (2.4G2, anti-CD16/32) for  
334 10 min at 4°C. Without wash, cells were then stained with fluorescence-tagged antibodies, such  
335 as mAbs to CD3 (145-2C11), CD8 (53-6.7), CD11c (HL3), CD11b (M1/70), CD25 (PC61),  
336 CD40 (3/23), CD44 (IM7), CD45.1 (A20), CD45.2 (104), CD62L (MEL-14), CD69 (H1.2F3),  
337 CD86 (GL1), CD103 (M290), CD127 (SB/199), Ly-6G (1A8) and Siglec-F (MR1) purchased  
338 from BD Biosciences and CD4 (GK1.5), CD39 (24DMS1), LFA-1 (M17/4), Ly-6C (HK1.4),  
339 MHC-II (I-A/I-E) (M5/114.15.2) and PD-1 (J43) purchased from eBiosciences, at 4°C for 20~30  
340 min. For intracellular staining of Foxp3, Ki67 and CTLA-4, cells were fixed in 1x  
341 Fixation/Permeabilization Buffer (eBiosciences) at 4°C for 45 min, followed by intracellularly

342 staining with mAbs to Foxp3 (MF23, BD Biosciences), Ki67 (SolA15, eBiosciences) or CTLA-4  
343 (UC10-4B9, eBiosciences) in 1x Permeabilization Buffer (eBiosciences) for at least 1 h at 4°C.  
344 For intracellular cytokine staining (staining for IFN- $\gamma$  and IL-10), cells were fixed in 1%  
345 paraformaldehyde (PFA) at RT for 30 min and then stained with mAbs to IFN- $\gamma$  (XMG1.2, BD  
346 Biosciences) or IL-10 (JES5-16E3, Biolegend) in PBS containing 0.2% saponin at 4°C for 30  
347 min. After being washed once with PBS, cell samples were resuspended 150  $\mu$ l FACS buffer and  
348 acquired on a FACSCanto II flow cytometer (BD Biosciences). Flow cytometry data were  
349 analyzed with FlowJo software (FlowJo VX).

350

### 351 *Cell sorting*

352 Cell sorting was performed using a FACS Aria III cell sorter (BD Biosciences). Memory CD4<sup>+</sup> T  
353 cells and CD8<sup>+</sup> T cells were FACS-sorted from the spleen and lymph node cells of memory  
354 C57BL/6 or Ly5.1 mice. Naïve and memory Tregs (nTregs and mTregs) were sorted from naïve  
355 and memory B6-Foxp3<sup>eGFP</sup> mice, respectively. Both nTregs and mTregs were CD4<sup>+</sup>CD25<sup>+</sup>  
356 Foxp3<sup>eGFP+</sup>; however, nTregs were CD44<sup>-</sup>CD62L<sup>+</sup> and mTregs were CD44<sup>+</sup>CD62L<sup>-/low</sup>. For some  
357 experiments, CD4<sup>+</sup>CD25<sup>+</sup>CD44<sup>-</sup>CD62L<sup>+</sup> nTregs and CD4<sup>+</sup>CD25<sup>+</sup>CD44<sup>+</sup>CD62L<sup>-/low</sup> mTregs  
358 were sorted from naïve and memory C57BL/6 mice, respectively, by staining with mAbs to CD4,  
359 CD25, CD44 and CD62L. The cells isolated from Ly5.1 mice were CD45.1<sup>+</sup> and those isolated  
360 from C57BL/6 and B6-Foxp3<sup>eGFP</sup> mice were CD45.2<sup>+</sup>.

361

### 362 *Adoptive cell transfer*

363 For *in vivo* Treg migration and proliferation analysis, FACS-sorted mTregs (1 x 10<sup>6</sup>,  
364 CD45.2<sup>+</sup>eGFP<sup>+</sup>) were co-transferred with nTregs (1 x 10<sup>6</sup>, CD45.2<sup>+</sup>eGFP<sup>-</sup>) into congenic Ly5.1  
365 mice via tail intravenous injection (i.v.), followed by intranasal infection with PR8 (70 pfu in  
366 30 $\mu$ l PBS) 12 h after co-transfer. For *in vivo* analysis of Treg function, nTregs (1.5~2 x 10<sup>6</sup>,  
367 CD45.2<sup>+</sup>eGFP<sup>-</sup>) or mTregs (1.5~2 x 10<sup>6</sup>, CD45.2<sup>+</sup>eGFP<sup>+</sup>) were i.v. transferred individually into  
368 congenic Ly5.1 recipient mice 12 h before intranasal PR8 infection.

369

370 *Generation of BMDCs*

371 2 x 10<sup>6</sup> bone marrow cells from naïve Ly5.1 or C57BL/6 mice were grown in complete medium  
372 supplemented with X-63-GM-CSF supernatant (containing granulocyte-macrophage colony-  
373 stimulating factor, GM-CSF) in 10 mm petri dish. Culture medium was replaced on day 3 and  
374 day 6. Bone marrow derived dendritic cells (BMDCs) were harvested on day 8 by collecting the  
375 nonadherent cells.

376

377 *In vitro suppression assay*

378 For *in vitro* suppression of T cell proliferation, the responder IAV-specific CD4<sup>+</sup> or CD8<sup>+</sup> T cells  
379 (CD45.1<sup>+</sup>) were labeled with 5 $\mu$ M CFSE and cultured with Treg cell populations (CD45.2<sup>+</sup>) at  
380 various ratios in the presence of irradiated PR8-infected BMDCs (CD45.2<sup>+</sup>). IAV-specific CD4<sup>+</sup>  
381 or CD8<sup>+</sup> T cell proliferation was measured by carboxyfluorescein-succinimidyl ester (CFSE)  
382 dilution on day 5 and day 4 of culture, respectively. For *in vitro* suppression of BMDC activation,  
383 nTregs, mTregs or IAV-specific CD4<sup>+</sup> T cells (1 x 10<sup>5</sup>, CD45.2<sup>+</sup>) or a mix of two populations  
384 (1:1 ratio) were cultured with BMDCs (5 x 10<sup>4</sup>, CD45.1<sup>+</sup>) in U-bottomed 96-well plates in the  
385 presence of PR8 (MOI=1). After 24 h, cells were harvested by treating with 5 mM EDTA, and  
386 the expression of CD40, CD86 and MHC-II on BMDCs were FACS-analyzed after staining with  
387 mAbs specific to CD45.1, CD11c, CD86, CD40, and MHC-II.

388

389 *Confocal microscopy*

390 FACS-sorted nTregs and mTregs were labeled with Cell Proliferation Dye eFluor™ 670 and  
391 CFSE, respectively, according to the manufacturer's instruction. Labeled nTregs and mTregs  
392 (1.5 x 10<sup>5</sup>) were cultured with non-labeled PR8-infected BMDCs (3 x 10<sup>4</sup>) in 8-well Lab-Tek™  
393 II Chambered Coverglass. Alternatively, labeled nTregs and mTregs (1.5 x 10<sup>5</sup>) were cultured  
394 with non-labeled BMDCs (3 x 10<sup>4</sup>) in the absence or presence of purified anti-CD3/anti-CD28  
395 mAbs (1  $\mu$ g mL<sup>-1</sup> and 0.5  $\mu$ g mL<sup>-1</sup>, respectively). Live cell imaging was performed to analyze  
396 Treg-BMDC aggregation after 12 h co-incubation with a Zeiss Confocal Spinning Disk  
397 microscope. Cells were monitored with 20x and 63x objectives for analysis of cell aggregation

398 and morphological change, respectively. During imaging, cells were maintained at 37°C and  
399 supplemented with 5% CO<sub>2</sub> to sustain their viability.

400

#### 401 *Histological analysis*

402 Recipient mice were adoptively transferred with nTregs or mTregs and infected with PR8 as  
403 previously described. Their lungs were collected on day 10 post infection and inflated with 1 mL  
404 PFA (4%, v/v) via the trachea and fixed for 16 h, at RT, followed by further fixation in 70%  
405 ethanol for 7 days at RT. Lungs were embedded in paraffin wax, and 5 mm sections were  
406 mounted onto slides and stained with H&E. All slides were imaged on a Nikon Eclipse  
407 microscope and captured images were analyzed by Fiji ImageJ software. The histology scores  
408 were assessed based on the infiltration rate calculated by Fiji ImageJ software.

409

#### 410 *Statistical analysis*

411 Statistical analysis was performed using Prism 8 (GraphPad Software). Data are presented as  
412 mean ± SEM unless otherwise noted. Significance calculations were determined by unpaired  
413 two-tailed Student's *t*-test for comparison between two groups or one-way ANOVA for multiple  
414 comparisons between different groups. A value of  $P > 0.05$  was deemed not statistically  
415 significant (ns); \* $P < 0.05$ , \*\* $P < 0.01$ , \*\*\* $P < 0.001$ , and \*\*\*\* $P < 0.0001$ .

416

#### 417 **ACKNOWLEDGMENTS**

418 This project was partly supported by the NHMRC Senior Research Fellowship 603104 to WC  
419 and the NHMRC program grant 567122.

420

#### 421 **CONFLICT OF INTEREST**

422 The authors declare no conflict of interest.

423

424 **REFERENCES**

- 425 1. Fontenot JD, Gavin MA, Rudensky AY. Foxp3 programs the development and function of  
426 CD4<sup>+</sup>CD25<sup>+</sup> regulatory T cells. *Nat Immunol* 2003; **4**: 330-336.
- 427 2. Josefowicz SZ, Lu LF, Rudensky AY. Regulatory T cells: mechanisms of differentiation and  
428 function. *Annu Rev Immunol* 2012; **30**: 531-564.
- 429 3. Wing K, Sakaguchi S. Regulatory T cells exert checks and balances on self tolerance and  
430 autoimmunity. *Nat Immunol* 2010; **11**: 7-13.
- 431 4. Sakaguchi S, Yamaguchi T, Nomura T, *et al.* Regulatory T cells and immune tolerance. *Cell* 2008;  
432 **133**: 775-787.
- 433 5. Grant CR, Liberal R, Mieli-Vergani G, *et al.* Regulatory T-cells in autoimmune diseases:  
434 challenges, controversies and--yet--unanswered questions. *Autoimmun Rev* 2015; **14**: 105-116.
- 435 6. Zemmour D, Pratama A, Loughhead SM, *et al.* Flicr, a long noncoding RNA, modulates Foxp3  
436 expression and autoimmunity. *Proc Natl Acad Sci U S A* 2017; **114**: E3472-E3480.
- 437 7. Carbone F, De Rosa V, Carrieri PB, *et al.* Regulatory T cell proliferative potential is impaired in  
438 human autoimmune disease. *Nat Med* 2014; **20**: 69-74.
- 439 8. Plaza-Sirvent C, Schuster M, Neumann Y, *et al.* c-FLIP expression in Foxp3-expressing cells is  
440 essential for survival of regulatory T cells and prevention of autoimmunity. *Cell Rep* 2017; **18**: 12-22.
- 441 9. Fulton RB, Meyerholz DK, Varga SM. Foxp3<sup>+</sup> CD4 regulatory T cells limit pulmonary  
442 immunopathology by modulating the CD8 T cell response during respiratory syncytial virus infection. *J*  
443 *Immunol* 2010; **185**: 2382-2392.
- 444 10. Lee DCP, Harker JAE, Tregoning JS, *et al.* CD25<sup>+</sup> natural regulatory T cells are critical in  
445 limiting innate and adaptive immunity and resolving disease following respiratory syncytial virus  
446 infection. *J Virol* 2010; **84**: 8790-8798.
- 447 11. Suvas S, Kumaraguru U, Pack CD, *et al.* CD4<sup>+</sup>CD25<sup>+</sup>T cells regulate virus-specific primary and  
448 memory CD8<sup>+</sup> T cell responses. *J Exp Med* 2003; **198**: 889-901.
- 449 12. Lund JM, Hsing L, Pham TT, *et al.* Coordination of early protective immunity to viral infection  
450 by regulatory T cells. *Science* 2008; **320**: 1220-1224.
- 451 13. Betts RJ, Prabhu N, Ho AW, *et al.* Influenza A virus infection results in a robust, antigen-  
452 responsive, and widely disseminated Foxp3<sup>+</sup> regulatory T cell response. *J Virol* 2012; **86**: 2817-2825.
- 453 14. Bedoya F, Cheng GS, Leibow A, *et al.* Viral antigen induces differentiation of Foxp3<sup>+</sup> natural  
454 regulatory T cells in influenza virus-infected mice. *J Immunol* 2013; **190**: 6115-6125.
- 455 15. Brincks EL, Roberts AD, Cookenham T, *et al.* Antigen-specific memory regulatory CD4<sup>+</sup>Foxp3<sup>+</sup>  
456 T cells control memory responses to influenza virus infection. *J Immunol* 2013; **190**: 3438-3446.

- 457 16. Huehn J, Hamann A. Homing to suppress: address codes for Treg migration. *Trends Immunol*  
458 2005; **26**: 632-636.
- 459 17. van der Veeken J, Gonzalez AJ, Cho H, *et al.* Memory of Inflammation in Regulatory T Cells.  
460 *Cell* 2016; **166**: 977-990.
- 461 18. Short KR, Kroeze E, Fouchier RAM, *et al.* Pathogenesis of influenza-induced acute respiratory  
462 distress syndrome. *Lancet Infect Dis* 2014; **14**: 57-69.
- 463 19. La Gruta NL, Kedzierska K, Stambas J, *et al.* A question of self-preservation: immunopathology  
464 in influenza virus infection. *Immunol Cell Biol* 2007; **85**: 85-92.
- 465 20. Antunes I, Kassiotis G. Suppression of innate immune pathology by regulatory T cells during  
466 Influenza A virus infection of immunodeficient mice. *J Virol* 2010; **84**: 12564-12575.
- 467 21. Moser EK, Hufford MM, Braciale TJ. Late engagement of CD86 after influenza virus clearance  
468 promotes recovery in a FoxP3<sup>+</sup> regulatory T cell dependent manner. *PLoS Pathog* 2014; **10**: e1004315.
- 469 22. Booth NJ, McQuaid AJ, Sobande T, *et al.* Different proliferative potential and migratory  
470 characteristics of human CD4<sup>+</sup> regulatory T cells that express either CD45RA or CD45RO. *J Immunol*  
471 2010; **184**: 4317-4326.
- 472 23. Thornton AM, Piccirillo CA, Shevach EM. Activation requirements for the induction of  
473 CD4<sup>+</sup>CD25<sup>+</sup> T cell suppressor function. *Eur J Immunol* 2004; **34**: 366-376.
- 474 24. Ochando JC, Yopp AC, Yang Y, *et al.* Lymph node occupancy is required for the peripheral  
475 development of alloantigen-specific Foxp3<sup>+</sup> regulatory T cells. *J Immunol* 2005; **174**: 6993-7005.
- 476 25. Fisson S, Darrasse-Jeze G, Litvinova E, *et al.* Continuous activation of autoreactive CD4<sup>+</sup>CD25<sup>+</sup>  
477 regulatory T cells in the steady state. *J Exp Med* 2003; **198**: 737-746.
- 478 26. Suffia I, Reckling SK, Salay G, *et al.* A role for CD103 in the retention of CD4<sup>+</sup>CD25<sup>+</sup> Treg and  
479 control of Leishmania major infection. *J Immunol* 2005; **174**: 5444-5455.
- 480 27. Huehn J, Siegmund K, Lehmann JC, *et al.* Developmental stage, phenotype, and migration  
481 distinguish naive- and effector/memory-like CD4<sup>+</sup> regulatory T cells. *J Exp Med* 2004; **199**: 303-313.
- 482 28. Teijaro JR, Walsh KB, Cahalan S, *et al.* Endothelial cells are central orchestrators of cytokine  
483 amplification during influenza virus infection. *Cell* 2011; **146**: 980-991.
- 484 29. D'Elia RV, Harrison K, Oyston PC, *et al.* Targeting the "cytokine storm" for therapeutic benefit.  
485 *Clin Vaccine Immunol* 2013; **20**: 319-237.
- 486 30. Liu Q, Zhou YH, Yang ZQ. The cytokine storm of severe influenza and development of  
487 immunomodulatory therapy. *Cell Mol Immunol* 2016; **13**: 3-10.
- 488 31. Julkunen I, Melen K, Nyqvist M, *et al.* Inflammatory responses in influenza A virus infection.  
489 *Vaccine* 2000; **19 Suppl 1**: S32-S37.

- 490 32. Fletcher JM, Lonergan R, Costelloe L, *et al.* CD39<sup>+</sup>Foxp3<sup>+</sup> regulatory T cells suppress pathogenic  
491 Th17 cells and are impaired in multiple sclerosis. *J Immunol* 2009; **183**: 7602-7610.
- 492 33. Ferrari D, Pizzirani C, Adinolfi E, *et al.* The P2X7 receptor: a key player in IL-1 processing and  
493 release. *J Immunol* 2006; **176**: 3877-3883.
- 494 34. McGill J, Van Rooijen N, Legge KL. Protective influenza-specific CD8 T cell responses require  
495 interactions with dendritic cells in the lungs. *J Exp Med* 2008; **205**: 1635-1646.
- 496 35. Matheu MP, Othy S, Greenberg ML, *et al.* Imaging regulatory T cell dynamics and CTLA4-  
497 mediated suppression of T cell priming. *Nat Commun* 2015; **6**: 7219.
- 498 36. Bolton HA, Zhu EH, Terry AM, *et al.* Selective Treg reconstitution during lymphopenia  
499 normalizes DC costimulation and prevents graft-versus-host disease. *J Clin Invest* 2015; **125**: 3627-3641.
- 500 37. Chen J, Ganguly A, Mucsi AD, *et al.* Strong adhesion by regulatory T cells induces dendritic cell  
501 cytoskeletal polarization and contact-dependent lethargy. *J Exp Med* 2017; **214**: 327-338.
- 502 38. Surls J, Nazarov-Stoica C, Kehl M, *et al.* Differential effect of CD4<sup>+</sup>Foxp3<sup>+</sup> T-regulatory cells on  
503 the B and T helper cell responses to influenza virus vaccination. *Vaccine* 2010; **28**: 7319-7330.
- 504 39. Lin PH, Wong WI, Wang YL, *et al.* Vaccine-induced antigen-specific regulatory T cells attenuate  
505 the antiviral immunity against acute influenza virus infection. *Mucosal Immunol* 2018; **11**: 1239-1253.
- 506 40. Tamura S, Aina A, Suzuki T, *et al.* Intranasal inactivated influenza vaccines: a reasonable  
507 approach to improve the efficacy of influenza vaccine? *Jpn J Infect Dis* 2016; **69**: 165-179.
- 508 41. Zens KD, Chen JK, Farber DL. Vaccine-generated lung tissue-resident memory T cells provide  
509 heterosubtypic protection to influenza infection. *JCI Insight* 2016; **1**: e85832.
- 510 42. Fontenot JD, Rasmussen JP, Williams LM, *et al.* Regulatory T cell lineage specification by the  
511 forkhead transcription factor FoxP3. *Immunity* 2005; **22**: 329-341.
- 512 43. Hou S, Doherty PC, Zijlstra M, *et al.* Delayed clearance of Sendai virus in mice lacking class I  
513 MHC-restricted CD8<sup>+</sup> T cells. *J Immunol* 1992; **149**: 1319-1325.

514

515

## 516 **Figure Legends**

517 **Figure 1.** mTregs exhibit distinct expression of peripheral migration- and suppression-associated markers. (a)  
518 nTregs (CD4<sup>+</sup>eGFP<sup>+</sup>CD44<sup>+</sup>CD62L<sup>+</sup>) and nmTregs (CD4<sup>+</sup>eGFP<sup>+</sup>CD44<sup>+</sup>CD62L<sup>-/low</sup>) from naïve B6-Foxp3<sup>eGFP</sup> mice  
519 and mTregs (CD4<sup>+</sup>eGFP<sup>+</sup>CD44<sup>+</sup>CD62L<sup>-/low</sup>) from memory B6-Foxp3<sup>eGFP</sup> mice were FACS-analyzed for their  
520 expression of a panel of surface and intracellular makers including CD25, CD39, CD69, CD103, CTLA-4, LFA-1,  
521 PD-1, and Foxp3. Histogram (b) and MFI (c) depict the expression of CD25, CD39, CD69, CD103, CTLA-4, LFA-  
522 1, PD-1, and Foxp3 by nTregs (grey), nmTregs (black dashed) and mTregs (black). Data represent one of three

523 independent experiments, each with  $n \geq 6$  mice per group. ns means not significant;  $*P < 0.05$ ;  $**P < 0.01$ ;  $***P <$   
524  $0.001$ ;  $****P < 0.0001$ .

525

526 **Figure 2.** mTregs are more responsive to IAV-infected APC than nTregs *in vitro*. nTregs and mTregs were FACS-  
527 sorted from naïve and memory B6-Foxp3eGFP mice, respectively, with  $n \geq 6$  mice per group. (a) Ki67 expressing  
528 cells among unstimulated or IAV-stimulated nTregs and mTregs. nTregs and mTregs were co-cultured with  
529 (stimulated) or without (unstimulated) PR8-infected BMDC for 72h followed by flow cytometric analysis of Ki67<sup>+</sup>  
530 cells. (b) Co-culture of nTregs and mTregs with PR8-infected BMDCs. A mixture (1:1 ratio) of nTregs (red) and  
531 mTregs (green) were co-cultured with PR8-infected BMDCs. 12 h after co-culture, a series of images was taken at 1  
532 min intervals. Yellow open and filled arrows trace two nTregs, respectively; and blue open and filled arrows trace  
533 two mTregs, respectively. Scale bars, 20,000nm. Data represent one of three independent experiments. ns means not  
534 significant;  $***P < 0.001$ .

535

536 **Figure 3.** IAV infection selectively triggers a vigorous activation, proliferation and migration of mTregs at and to  
537 the infection site. (a and b) Experimental design schematic (a) and flow cytometric gating strategy (b). nTregs and  
538 mTregs were FACS-sorted from naïve C57BL/6 and memory C57BL/6-Foxp3<sup>eGFP</sup> mice, respectively, and then 1:1  
539 co-transferred into naïve Ly5.1 mice. Flow cytometric gating strategy for analyzing the frequency and total number  
540 of transferred nTregs and mTregs from the recipient mice at 10 dpi. Tregs from the recipient mice were gated by  
541 using a Foxp3<sup>+</sup>CD25<sup>+</sup> gate followed by identification of the adoptively transferred nTregs and mTregs based on the  
542 expression of congenic markers, CD45.1, CD45.2, and the reporter green fluorescent protein, eGFP. (c) The  
543 frequency of Ki67<sup>+</sup> cells within the adoptively transferred nTregs and mTregs in the spleens, pLNs, mLNs, BALs  
544 and lungs of recipients at 10 dpi. (d and e) The frequency (d) and total number (e) of the adoptively transferred  
545 nTregs (eGFP<sup>-</sup>; grey symbols) and mTregs (eGFP<sup>+</sup>; black symbols) in the spleens, pLNs, mLNs, BALs and lungs of  
546 recipients at 9 dpi. Data are representative of three independent experiments, each with  $n = 5$  mice per group. ns  
547 means not significant;  $*P < 0.05$ ;  $**P < 0.01$ ;  $***P < 0.001$ ;  $****P < 0.0001$ .

548

549 **Figure 4.** mTregs display enhanced suppression on the proliferation of IAV-specific CD4<sup>+</sup> and CD8<sup>+</sup> T cells. (a and  
550 b) *In vitro* proliferation of unstimulated or PR8-infected BMDCs-stimulated IAV-specific CD4<sup>+</sup> (a) and CD8<sup>+</sup> (b) T  
551 cell lines. The proliferation of IAV-specific CD4<sup>+</sup> and CD8<sup>+</sup> T cells were assessed by CFSE dilution on day 5 and  
552 day 4 after co-culture, respectively. Histograms show the CFSE dilution in both unstimulated and stimulated IAV-  
553 specific CD4<sup>+</sup> and CD8<sup>+</sup> T cells (a and b, left panels). The proliferation rates show the percentage of cells that had  
554 diluted CFSE (a and b, right panels). (c) *In vitro* suppression of IAV-specific CD4<sup>+</sup> and CD8<sup>+</sup> T cell proliferation by  
555 nTregs and mTregs. IAV-specific CD4<sup>+</sup> (left panel) and CD8<sup>+</sup> (right panel) T cells were co-cultured with graded  
556 nTreg (grey dashed lines) or mTreg (black dashed lines) numbers in the presence of PR8-infected BMDCs. The

557 suppression on the proliferation of IAV-specific CD4<sup>+</sup> and CD8<sup>+</sup> T cells by nTregs or mTregs were assessed on day  
558 5 and day 4 after co-culture, respectively. The suppression rate represents the capacity of nTregs or mTregs to  
559 inhibit the proliferation of IAV-specific CD4<sup>+</sup> and CD8<sup>+</sup> T cells. Data represent one of three independent  
560 experiments. \**P* < 0.05; \*\**P* < 0.01; \*\*\**P* < 0.001; \*\*\*\**P* < 0.0001.

561  
562 **Figure 5.** mTregs actively down-regulate CD40 and CD86 expression on BMDCs. **(a and b)** Expression of CD40  
563 and CD86 on BMDCs. Immature BMDCs were co-cultured with CD4<sup>+</sup> T cells or a mix of two populations (CD4<sup>+</sup>  
564 T/nTregs or CD4<sup>+</sup> T/mTregs) at a 1:1 ratio for 24 h in the presence of IAV followed by flow cytometric analysis of  
565 CD40 and CD86 expression. As the control, immature BMDCs alone were also cultured in the presence of IAV  
566 under the same conditions. Histograms **(a)** and bar graphs **(b)** show the expression and MFI of CD40 and CD86.  
567 Data represent one of three independent experiments. \**P* < 0.05; \*\*\*\**P* < 0.0001.

568  
569 **Figure 6.** Adoptive transfer of mTregs, but not nTregs, prior to IAV infection results in marked attenuation in  
570 infection-induced body weight loss and lung damage. nTregs or mTregs were adoptively transferred into Ly5.1  
571 recipient mice 12 h before intranasal PR8 infection. **(a)** Body weight of PBS-injected (Control), PR8-infected  
572 (Infected only), adoptively transferred nTregs plus PR8-infected (Infected + nTregs) and adoptively transferred  
573 mTregs plus PR8-infected (Infected + mTregs) mice. Body weight changes were monitored daily after PR8 infection.  
574 Depicted *P*-value corresponds to comparison of “Infected only” with “Infected + mTregs”. The difference between  
575 “infected only” and “Infected + nTregs” was not statistically significant. These data are representative of more than  
576 three independent experiments. **(b and c)** Histopathological analysis of the lungs from control, infected only,  
577 “Infected + nTregs” and “Infected + mTregs” mice on day 10 post PBS or PR8 inoculation. **(b)** Representative H&E  
578 stained histological lung tissue sections. **(c)** Quantification of infiltration rate (left) measured by Fiji imageJ and  
579 extent of tissue damage (right) scored according to infiltration rate. These data represent one of three independent  
580 experiments (n ≥ 5 mice per group). ns means not significant; \**P* < 0.05; \*\**P* < 0.01; \*\*\**P* < 0.001; \*\*\*\**P* < 0.0001.

581  
582 **Supplementary figure 1.** mTregs are bigger in size and making more contact with IAV-infected BMDCs. nTregs  
583 and mTregs were FACS-sorted from naïve and memory B6-Foxp3<sup>eGFP</sup> mice, respectively, with n ≥ 6 mice per group.  
584 **(a and b)** A mixture (1:1 ratio) of nTregs and mTregs were co-cultured with PR8-infected BMDCs. 12 h after co-  
585 culture, a series of images was taken at 1 min intervals, followed by quantitating cell size **(a)** and average Treg-DC  
586 contacting time **(b)** were analyzed using Fiji ImageJ software. Data represent one of three independent experiments.  
587 ns means not significant; \**P* < 0.05; \*\**P* < 0.01; \*\*\**P* < 0.001.

588  
589 **Supplementary figure 2.** nTregs and mTregs activation triggered by anti-CD3/CD28 antibodies. Ki67 expressing  
590 cells among unstimulated or anti-CD3/CD28 antibodies-stimulated nTregs and mTregs. nTregs and mTregs were

591 co-cultured with BMDCs for 72h in the absence or presence of anti-CD3/CD28 antibodies prior to the flow  
592 cytometric analysis of Ki67<sup>+</sup> cells. Data represent one of three independent experiments. ns means not significant.

593

594 **Supplementary figure 3.** mTregs are activated to proliferate and migrate *in vivo* specifically by IAV infection.  
595 1x10<sup>6</sup> FACS-purified mTregs from memory C57BL/6-Foxp3<sup>eGFP</sup> mice were adoptively transferred into congenic  
596 Ly5.1 mice. The recipient mice were intranasally inoculated with PBS or PR8 and sacrificed on day 10 post PBS- or  
597 PR8-inoculation. **(a)** The percentage of Ki67<sup>+</sup> cells among the adoptively transferred total mTregs recovered in the  
598 spleens, pLNs, mLNs and lungs of PBS treated (black symbols) or PR8 infected (grey symbols) recipients. **(b)** Total  
599 number of adoptively transferred mTregs in the spleens, pLNs, mLNs and lungs of PBS treated or PR8 infected  
600 recipients. Data are representative of three independent experiments, each with n ≥ 4 mice per group. ns means not  
601 significant; \*P < 0.05; \*\*P < 0.01; \*\*\*P < 0.001; \*\*\*\*P < 0.0001.

602

603 **Supplementary figure 4.** IAV infection and co-culture with nTregs or mTregs does not result in marked change in  
604 the expression of CD40 and CD86 on BMDCs. **(a and b)** Expression of CD40 and CD86 on IAV-infected BMDCs.  
605 Immature BMDCs were cultured in the absence or presence of IAV for 24 h; alternatively, immature BMDCs were  
606 co-cultured with nTregs or mTregs in the presence of IAV for 24 h; the expression of CD40 and CD86 on BMDCs  
607 were then FACS-analyzed. Histograms **(a)** and bar graphs **(b)** show the expression and MFI of CD40 and CD86.  
608 Data are representative of three independent experiments. ns means not significant.

609

610 **Supplementary figure 5.** mTregs actively limit the infiltration of monocytes, neutrophils and IFN-γ-secreting CD4<sup>+</sup>  
611 and CD8<sup>+</sup> T cells into the infected lungs. nTregs or mTregs were adoptively transferred into Ly5.1 recipient mice 12  
612 h before intranasal PR8 infection. Ly5.1 recipient mice were sacrificed at 10 dpi and cells in the lungs were isolated  
613 and stained for monocytes (CD11b<sup>+</sup>Ly6C<sup>+</sup>), interstitial macrophages (CD11b<sup>+</sup>Siglec-F<sup>low/-</sup>) and neutrophils  
614 (CD11b<sup>+</sup>Ly6G<sup>+</sup>). Alternatively, the IFN-γ-secreting CD4<sup>+</sup> (CD4<sup>+</sup>Foxp3<sup>-</sup>INF-γ<sup>+</sup>) and CD8<sup>+</sup> (CD8<sup>+</sup>INF-γ<sup>+</sup>) T cells  
615 were analyzed after peptide stimulation. **(a-e)** Total number of infiltrating monocytes **(a)**, interstitial macrophages  
616 **(b)**, neutrophils **(c)**, IFN-γ-secreting CD4<sup>+</sup> **(d)** and CD8<sup>+</sup> **(e)** T cells in the lungs of PBS-injected (Control), PR8-  
617 infected (Infected only), adoptively transferred nTregs plus PR8-infected (Infected + nTregs) and adoptively  
618 transferred mTregs plus PR8-infected (Infected + mTregs) mice. Data are representative of three independent  
619 experiments (n ≥ 4 mice per group). ns means not significant; \*P < 0.05; \*\*P < 0.01; \*\*\*P < 0.001; \*\*\*\*P < 0.0001.



**Figure 2**

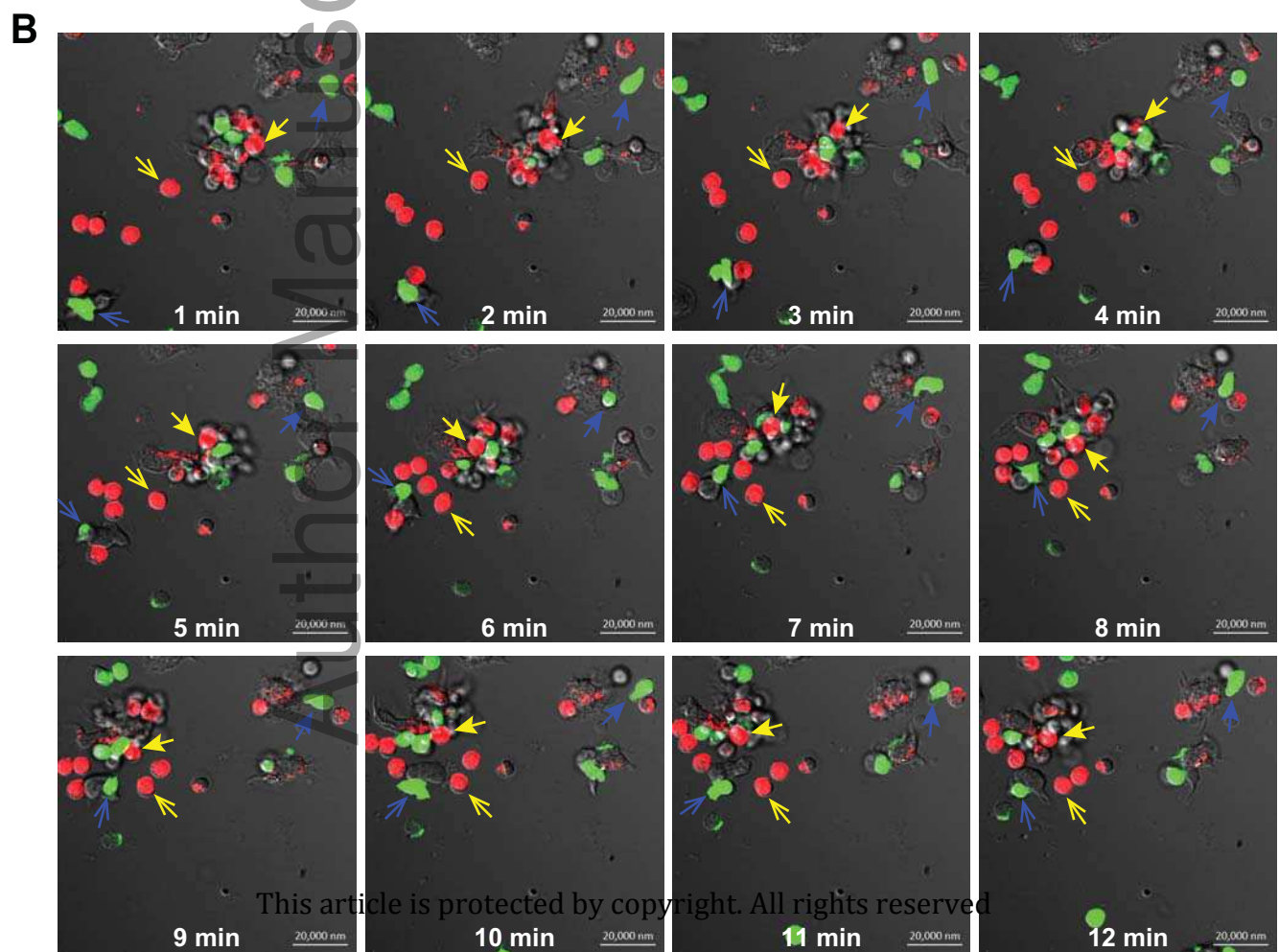
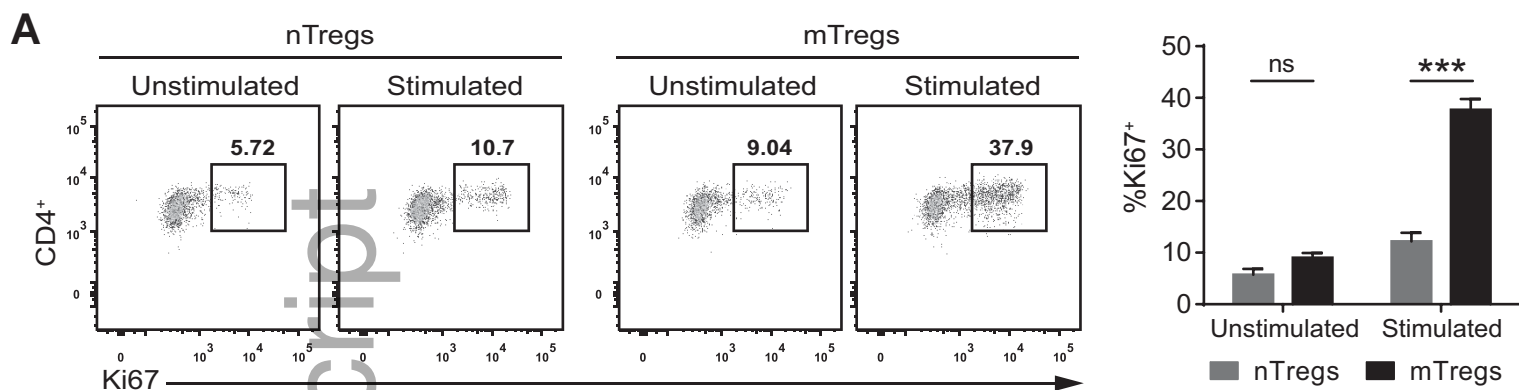


# Figure 3

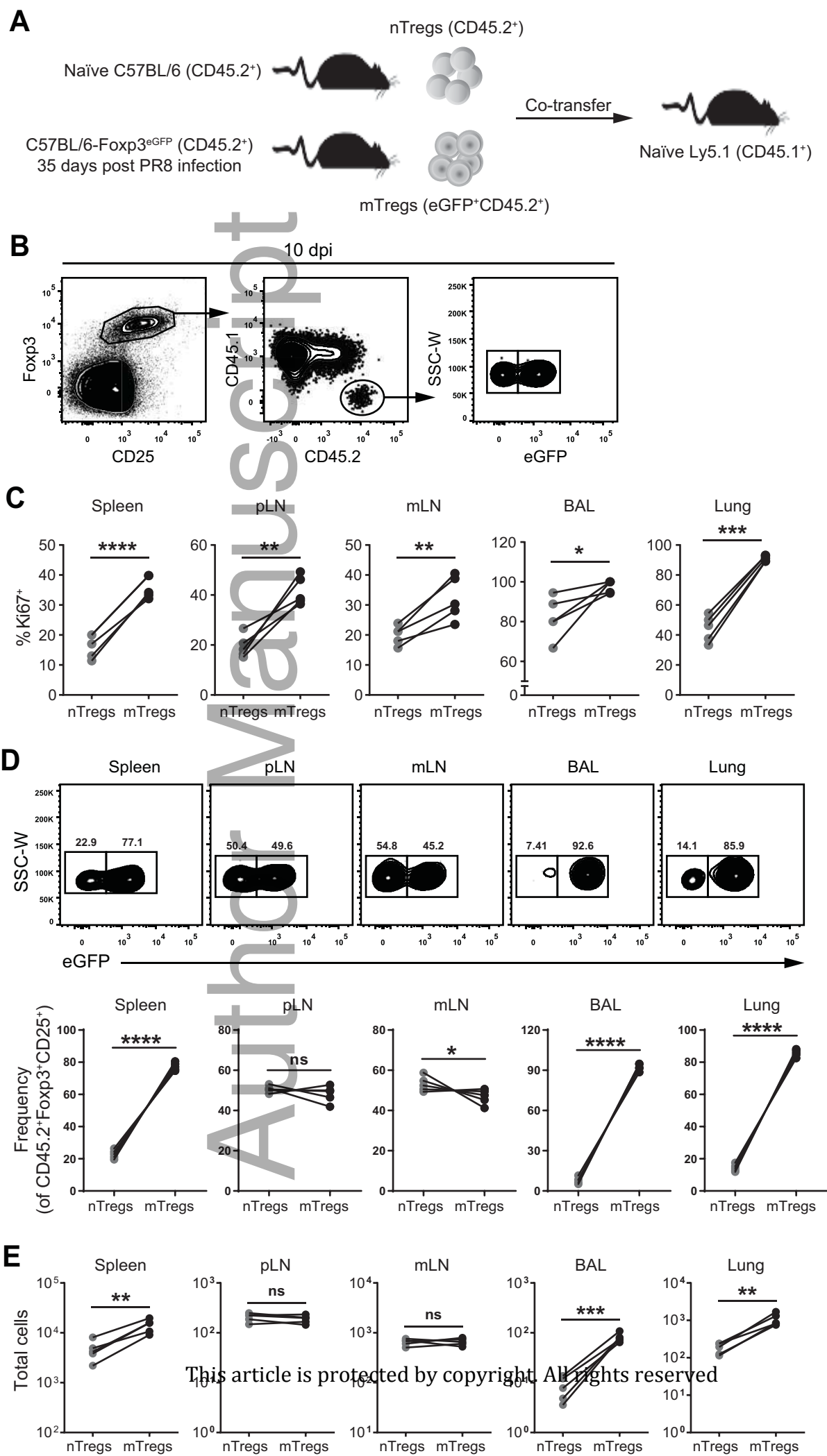
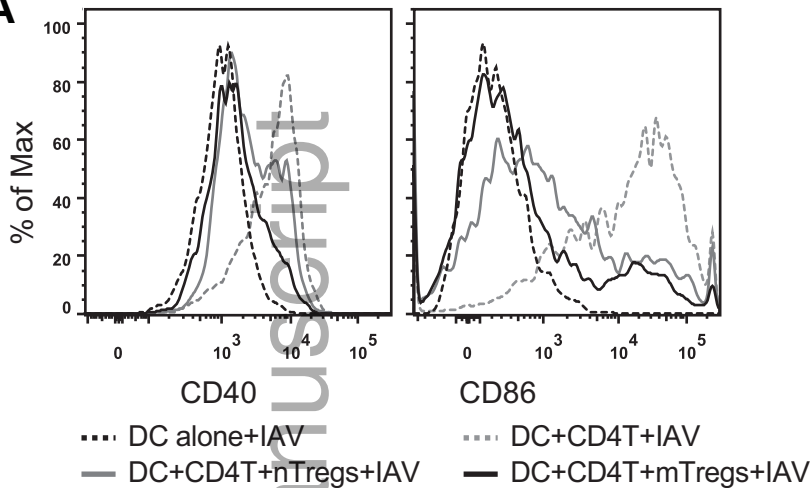


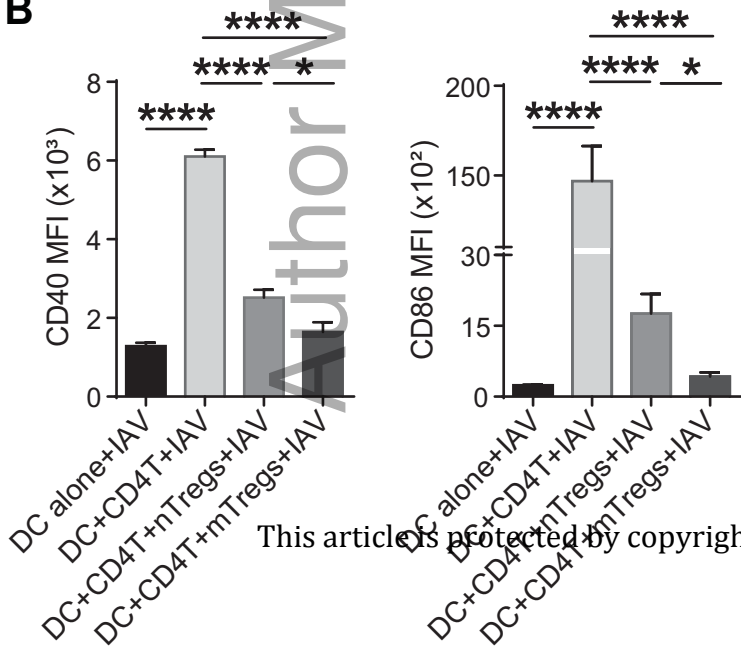


# Figure 5

**A**



**B**



This article is protected by copyright. All rights reserved.

**Figure 6**